Prod. Eng. Res. Devel. (2013) 7:517–525
DOI 10.1007/s11740-013-0479-x

MACHINE TOOL

Development of a pantograph based micro-machine for nano-scratching

Shishir Kumar Singh · Aneissha Chebolu · Soumen Mandal · Nagahanumaiah

Received: 21 February 2013 / Accepted: 11 May 2013 / Published online: 26 May 2013

Abstract Micro-nano patterned surfaces possess unique adhesion, wetting and dewetting properties, prompting their growing applications ranging from water repellant windshields of automobiles, antibacterial surfaces of medical devices to algae cultivation for biodiesel generation. The current need is manufacturing systems and processing protocols to create highly controlled patterns directly on solid substrates over large area. In this paper, a pantograph-based desktop micro machine has been designed to create micro-nano scale patterns over 25 mm × 25 mm area directly over solid surfaces by nano-scratching/scribing process. It is designed to achieve precision positioning of scratching tool (tip) and to retain its orientation such that effective rake angle remains unaltered, unlike in atomic force microscopy based scratching techniques. The design of the mechanism and micro-motion analysis achieved by integrating unique design for revolute joints are described. The machine performance in generating micro-patterns over copper and aluminium substrates has been studied.

Keywords Micro machine · Pantograph · Nano-scratching · Micro motion · Micro-nano patterning

1 Introduction

In micro nano systems engineering, the demand for manufacturing of highly controlled patterns directly on solid substrates such as metals, ceramics, glass, etc. over large area is continuously growing. This is owing to the unique properties of micro-nano patterned surfaces for corrosive resistance, antibacterial, hydrophobic, hydrophilic, reflective and refractive manipulations that attribute to their increasing deployment in several new generation applications ranging from water repellant windshields of automobiles to algae cultivation farms for biodiesel generation [1]. It needs to be appreciated that wide spread application of micro-nano patterned surfaces indispensably demands an innovative ultra-precision machine tool and processing protocols.

There have been multiple processes and substrate materials utilized for development of these patterned surfaces. The most commonly used techniques include photolithography, micro-molding and Focused Ion Beam (FIB) machining. Unfortunately, majority of these processes would become disadvantageous when looking for alternatives to produce micro-nano scale patterns of desired geometries directly over surfaces of metals, ceramics and other solid substrates. For example, lithography based processes need a mask, thus they are ineffective for patterning non-planar surfaces and for three dimensional features. Replica molding uses softer material and it needs patterned molds that restricts its use to laboratory experiments. FIB machining though relatively versatile, is highly expensive and is a slow process that makes it unsuitable for bulk integration.

On the other hand, mechanical based micro-nano fabrication techniques such as scratching; milling, EDM and pulsed laser processing have been applied to generate micro-nano patterns directly over an array of materials. While there is a better control over the shape and z-dimensions in laser machining, micro-milling and micro-EDM, these impose several challenges with respect to

S. K. Singh · A. Chebolu · S. Mandal · Nagahanumaiah (✉)
Micro Systems Technology Laboratory, CSIR—Central Mechanical Engineering Research Institute, M.G. Avenue, Durgapur 713209, West Bengal, India
e-mail: naga@cmeri.res.in; nagahanumaiah@gmail.com

Table 1 Comparative evaluation of various micro-nano patterning techniques

Process	Feature resolution	Material compatibility	Maturity level
Photolithography	~3 μm	Resists, functional organics	In production
Optical soft lithography	~90 nm	Resists, functional organics	Research
Embossing	~1 nm	Moldable resists,	In production
Hard imprint lithography	<10 nm	Organics, moldable resists,	Early production
Soft imprint lithography	<10 nm	Organics, moldable resists,	Research
Laser machining	~5 μm	Organics, semiconductors, conductors	Early production

cutting tool geometry, machine design and process control [2]. Moreover, many of the current nano fabrication process capabilities leave a lot to be desired, in terms of feature size, range of material, accuracy, reproducibility and in their maturity levels (Table 1).

1.1 Nano-scratching: challenges and opportunities

In literature, AFM-based nano-scratching has been widely employed for scribing grooves (<100 nm) over materials like Al, Ni, Si, SiO_2 using diamond tipped and diamond coated silicon at scribing speed ranging from 0.006 to 1.2 mm/min [3]. The relative motion between the AFM tip and the workpiece removes the material in few nanometers thickness. Although, tool load is controlled by measuring the deflection of cantilever, effective cutting forces depend significantly on tool geometry that is being altered with increasing deflection. As shown in Fig. 1, the effective rake angle keeps varying with cutting depth resulting in inconsistency in the quality of cut surfaces. For example, in Fig. 1, due to the deflection of cantilever from position a to position b, the tool orientation with respect to work surface changes that results in change in cutting geometry. Moreover, the scribing length is typically between a few microns to tens of micron in AFM-based scratching [3]. Short scribing lengths combined with low cutting speed makes AFM-based scratching low productivity process.

Nano-scratching process is emerging as a promising nano-machining process. The tool tips structured through FIB machining enables creation of complex patterns over a range of materials to a dimension scale as small as 10 nm. This process has significant potential to be uses as a production process, but it demands design of dynamically and thermally stable machine tool structure to be able to machine a micro-nano structure over a large work area [4]. In order to meet such demands of large area micro-nano patterning with complex geometries, a new class of micro machine which has minimum motion errors (resolution, positioning and repeatability), and structural errors (Abbe offset, thermal deformation, stiffness response) over long travel range is proposed. In this paper, a desktop micro machine has been designed to create micro-nano scale patterns over 25 mm × 25 mm area directly over metallic surfaces by nano-scratching/scribing process. In this micro machine, a pantograph based mechanism has been designed to achieve precision positioning of scratching tool (tip) and to retain the orientation of tip such that effective rake angle remains unaltered, unlike in atomic force microscopy (AFM) based scratching techniques.

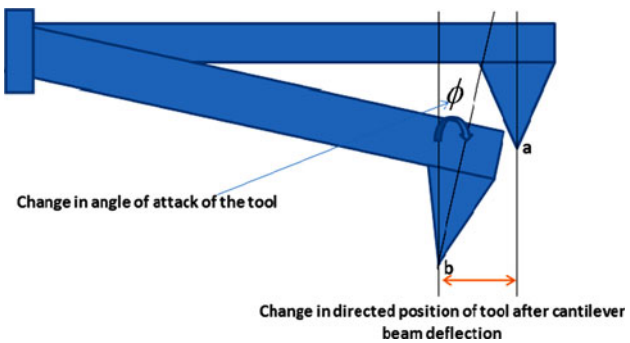

Fig. 1 Changed tool orientation in AFM based nano-scratching

2 Design methodology

In this research, authors worked towards the development of a micro machine designed for generating micro-nano scale patterns on metallic surfaces. The machine is based on contact based material removal mechanism where a tool with a pointed diamond tip scribes over the surface of metal. In order to impart the motion of tool tip in 100 nm resolution and also to keep the orientation of scratching tip unaltered over a scanning area of 25 mm × 25 mm, authors have investigated two design configurations. The first design is by integrating micro-positioning linear stages with 100 nm travel resolution over a range of 50 mm configured into 3-axis interpolation that resembles micro-planing. The second design is a pantograph based mechanism. Here, the motion is scaled down to 1/4 by the pantograph design. While, this paper is focused on the detailed design, motion analysis, and machining performance of pantograph based machine, the first design configuration and its performance in micro-scratching are delineated in order to establish background context.

2.1 Micro-planing based design

In this configuration, authors have developed a laboratory setup shown in Fig. 2, for micro-scratching that resembles micro-planing. This setup integrates micro-positioning stages with a travel resolution of 100 nm, configured to impart 50 mm travel along the X, Y and Z axis, controlled by customized multi-axis controller built over LabView platform. As an alternative to tool mounting over a cantilever in AFM, in this system a tungsten carbide tool with front rake angle of 8° and clearance angle of 5° was mounted over Z-axis stage. The depth of cut for grooves to be machined is set by adjusting the downward movement of Z-axis travel. The X-axis travel imparts movement of work piece against the tool that removes the material during its forward stroke. In order to create wider grooves and/or an array of parallel grooves, Y-axis travel was used intermittently. Using this setup grooves with width as low as 20 μm were produced to a depth of 30 μm over amorphous bulk metallic glass ($Zr_{24}Ti_{42}Cu_{15\cdot5}Ni_{14\cdot5}Br_{4.0}$.). The micro analysis of chips performed under optical microscope shows the formation of curled chips that clearly defines ductile mode of micro cutting.

The micro analysis of the grooves generated by this method indicates significant chatter marks. This is attributed to change in machine stiffness response and jerks induced by stepper motors used in linear stages. In addition, the major challenges with this setup for nano-scratching include precision positioning of tool tip, and the errors induced due to non-symmetrical structural configuration (w.r.t cutting point). While this design configuration set-up was successfully used to create 20 μm size scratches over 25 mm long with scratch width error of ±10 %, this design highlights few design challenges for nano-patterning that calls for new design configuration based on pantograph mechanism, used for tool tip motion control. On the other hand this experience helped authors to identify the design requirements discussed below and these have been taken care of in the second design configuration apart from incorporating targeted features: precision positioning of tool tip and maintaining effective rake angle irrespective of cutting depth.

It has been observed that design of the precision machine demands stable machine tool structure which can be achieved through a suitable structural design. Structural design is driven by the factors like symmetric structure, high rigidity, application of suitable new structural material and independent metrology frame of the machine. The proposed machine is designed in such a manner that center of gravity of the whole system is at minimum distance from the base so as to keep the potential energy of the system at a minimum. The second aspect is related to system integration to eliminate errors caused by control driven sources like active vibration, thermal deformation and it also requires to be isolated from the environment. In the proposed pantograph based design configuration, authors mainly focused on symmetry of the system and minimum number of contacts based design.

2.2 Pantograph based micro machine

A pantograph based mechanism which could scale down the motion of the actuator in order to enhance the precision in nano meter scale has been designed and is shown in Fig. 3. The structural design has been carefully carried out considering symmetry related issues, so that the machining point is located at the centroid of the entire system. The principal subsystems of this machine include a pantograph based mechanism for precision positioning of the tool tip, actuator to drive the pantograph, precision X–Y linear positioning stage, modular machine structure and control system interfaced with PC with a machine footprint of 240 mm × 200 mm × 300 mm.

The pantograph mechanism (Fig. 4) is capable of reducing the vertical travel range of piezo-actuator (∼180 μm) to nanometer range. It also positions the scratching tip attached to the Arm-E, over the targeted workpiece surface along Z-axis and keeps the orientation

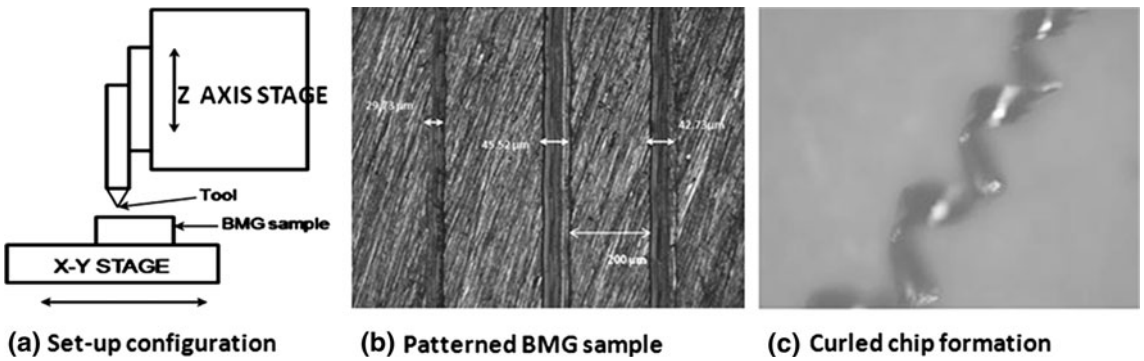

Fig. 2 Scratching over BMG using a system configured like micro-scale planning

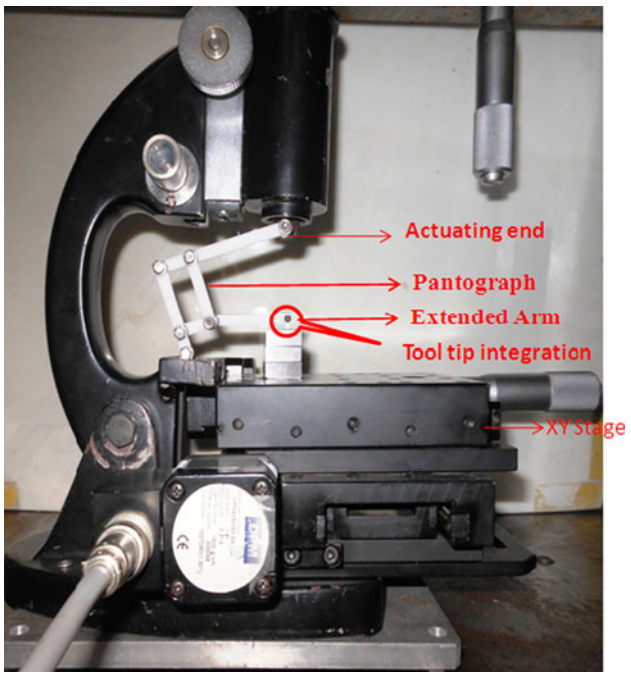

Fig. 3 Pantograph based micro machine prototype

of tool tip unaltered. Arm-E is connected to the pantograph at the point D having extension of the linear revolute joint shaft which is not allowed to rotate, thereby restricting the arc movement of tool tips mounted. The piezo actuator used is Physik Instrumente GmbH make of Model P-016.90 P for imparting Z-axis movement. It is connected to Arm-Q that provides a linear actuation at the point of attack and has a travel range of 180 µm. Arm-Q is connected to piezo actuator rigidly with the help of press fit slotted cap as shown in Fig. 4. This motion is transferred to the tracing point D (Arm-E) at reduced scale which can be adjusted by changing the magnification factor. The transfer of high blocking force generated by the piezo actuator to tool tips enables the scratching of harder surfaces.

A rack and pinion arrangement is used to adjust the coarse movement of the chip carrier up to 30 mm. A linear X–Y stage with travel range of 50 mm, 25 mm on either side of the reference axis (normal Z-axis) is used to provide lateral and transverse movement to the workpiece. In this work authors used Physik Instrumente GmbH made stacked piezo actuator (Model P-016.90 P). This actuator was driven by the PICA controller purchased from the same vendor. This integrated system has been used for controlling the movement of piezo actuator. In this micro machine, the requirement of piezo actuator is for precision positioning of tool tip in z- direction to set depth of cuts in nanometers resolution. Once the tool position has been set through pantograph mechanism, the scratches can be created by controlling travel in X-axis and Y-axis travel for width control and also for creating parallel scratches. Authors used LabView interface to achieve this synchronized motion control. Simulation results confirm the effective transfer of piezo blocking force to the tool tip which is sufficient to scribe the hard surface and scale down the motion of Piezo actuator up to nanometers for precision position of tool tip. These simulation studies were performed by considering the linear revolute joint without considering the effect of elasticity of pantograph. The pantograph mechanism design, micro motion analysis and performance of machine tool in nano-scratching over copper and aluminum substrates are discussed in the following sections. Kinematic and dynamic analysis was done using MSC Adams software to analyze the feasibility of the design.

2.3 Pantograph for nano-positioning

Literature reports many mechanisms to scale displacement obtained from actuators. Most commonly used ones for micro nano scale manipulation include flexural [5] and compliant mechanisms [6]. While the former suffers from issues related to flexural rigidity and stiffness, the latter faces relative difficulty in analyzing and designing compliant mechanisms. Due to the requirement of precision combined with the need of force restraining ability and structural rigidity of the scaling mechanism, the authors designed a modified pantograph based mechanism which eventually suits the objective.

In this micro machine, a pantograph based mechanism; driven by a piezo actuator having maximum travel of 180 µm at 100 nm resolution with a scaling factor of 1/4 has been designed. The performance of this mechanism in such precision applications depends heavily on accurate nano positioning of various links and joints. Therefore, development of such mechanism based device needs miniature components and precise linear travel and positioning of the systems.

Pantograph mechanism used in this machine has one degree of freedom (DOF), which is a well-known means for generating straight line motion in leg mechanism used in robotics (Fig. 5). It also provides kinematic linearity between input and output motion and introduces amplification factor between input motion and output motion. Finally, pantograph linearly decouples input–output motions. Moreover, this closed loop mechanism usually has advantageous static and dynamics characteristics [7]. The ordinary pantograph and skew pantograph is already used for linear actuation in robotics but is not applied for micro and nano scale actuation. 1DOF Pantograph based schematic diagram is shown in Fig. 5 which solves the problem of cantilever deflection and change in tool tip orientation. The designed pantograph has been further optimized to satisfy the footprint constraint of the micro

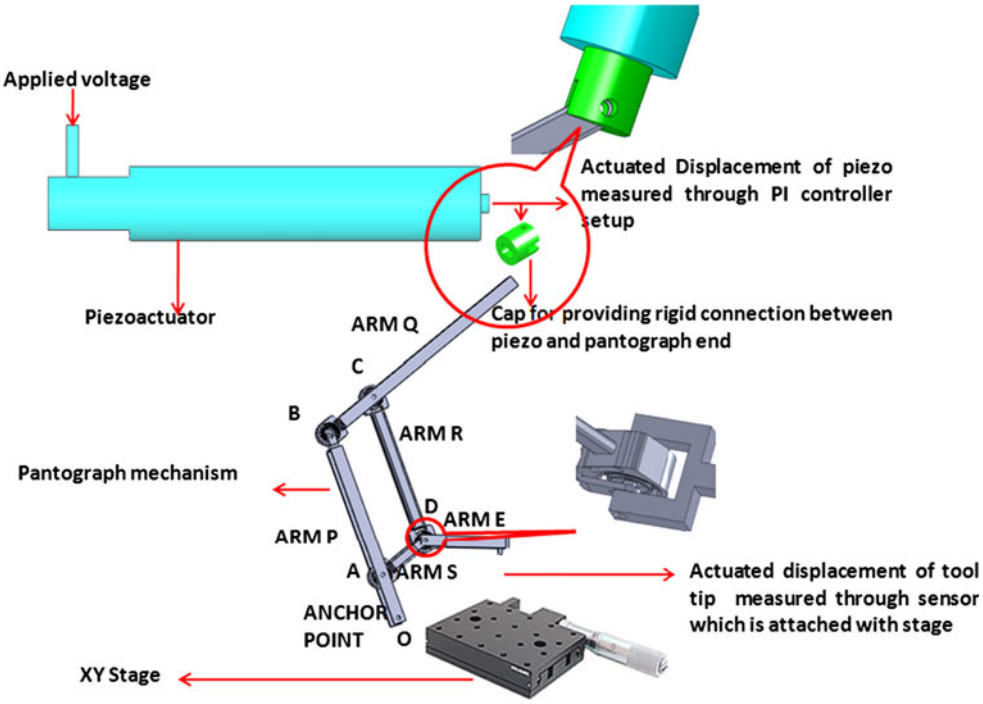

Fig. 4 Structural Configuration a pantograph based micro machine

machine and to achieve proper displacement scaling factor. This was facilitated using Lagrangian multiplier based optimization methodology as explained in the next section.

2.4 Design specification of pantograph

In the pantograph mechanism as shown in Fig. 5, links are such that AB||CD and AD||BC. It also satisfies one more condition which is given as

$$\frac{OB}{OA} = \frac{BE}{BC} = \frac{OE}{OD} = R$$

where R is a constant and for this design its value is 4, in order to scale down the actuator motion by 4 times. The dimension of pantograph is optimised using the Lagrange multiplier.

Since position of different joint is continuously varying in pantograph actuation, we took a particular value from CAD design model within an operating limit to avoid the singularity condition.

For example, If

$$\angle OBE = 90^\circ \text{ and } \angle XOB = \theta^\circ$$

Hence to avoid the singularity condition and for providing a better proportionate link to fit properly in compact space, the following equation is estimated for right angled triangle *OBE* which is forming a pantograph closed loop.

$$OB^2 + BE^2 = K \quad (1)$$

where K is a constant and its value depends upon the compact design space and the lengths of the links of the pantograph. While designing for optimised limiting range, its value is found to be 110 mm. In generalised co-ordinate system the above equation can be written as

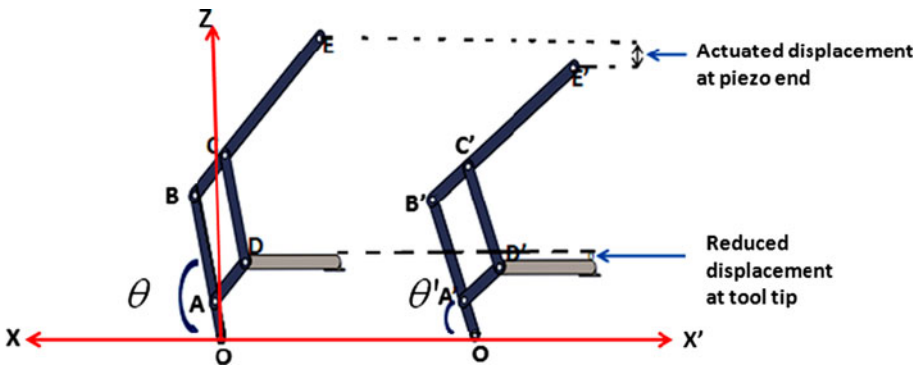

Fig. 5 Pantograph design reference diagram and actuation of pantograph for reduced scale

$$x^2 + z^2 = K \tag{2}$$

Since $m = \tan\theta$, for the link OB, one can easily write

$$z + mx = 0 \tag{3}$$

Using Lagrange multiplier, we can combine equation (2) and (3) as:

$$(x^2 + z^2 - K) + \lambda(z + mx) = 0 \tag{4}$$

Taking the partial derivative of above equation with respect to *x*, *z* and λ respectively

$$2x + \lambda\sqrt{3} = 0$$
$$2z + \lambda = 0$$
$$z + mx = 0$$

By solving the above equations x, z and λ can be obtained in terms of m. After solving these equations by trial and error, the length of proportionate links are optimised as given below.

OA = 13.75 mm
AB = CD = 41.15 mm
BC = AD = 23.8156986 mm
BE = 95.26279442 mm

2.5 Revolute joint design

Under tension–compression load cycling, conventional pin-clevis joints exhibit four types of nonlinear load–displacement response (a) free play due to clearances between the pin, tang, and clevis; (b) changes in stiffness due to the nonlinear contact between the pin, tang, and clevis; (c) unequal tension and compression stiffness (referred as bilinearity) due to different tension and compression load paths through the clevis and the tang; and (d) hysteresis due to friction between the joint components [8]. Current mathematical models of nonlinear joint phenomena involve numerous empirical parameters whose values are highly dependent on specific test conditions. To overcome the limitation of conventional revolute joint, authors adopted the linear revolute joint developed by NASA Langley Research Centre, USA [8] with certain modifications to suit the pantograph mechanism used in this micro machine.

As the revolute joint design given by NASA Langley Research Centre is larger than the size specifications of the micro machine, the design was modified so that it can be implemented in compact space. Figure 6 shows the modified linear revolute joint designed following the basic design proposed in [8]. The bearing (with ID = 6 mm, OD = 10 mm and ball diameter = 0.6 mm) assembly, shown in Fig. 6, consists of a hub and preload plate which retain and preload a commercially manufactured pair of precision bearings. The hub is machined with an outer diameter that makes a slip-fit with the inner race of the bearing. A raised lip is machined on the outer surface of the hub to retain the inner race of one bearing and to resist the preloading force applied by the preload plate, through the other bearing. The preload plate is attached to the hub using four small machine screws. As these screws are tightened, the outer lip of the preload plate makes contact with the inner race of one of the bearings. The clamping force generated by the four machine screws is applied solely to the inner races of the bearings, thus preloading the bearings according to the bearing manufacturer's specifications. A thin film liquid adhesive is applied between the inner bearing races and the hub to insure intimate contact and to eliminate any potential for free-play.

For designing this revolute joint, micro-lurching and micro-slippage effects have been neglected owing to low load actuation for small link length. However, effect of friction induced due to contact between bearing balls has been considered for the analysis. Figure 7 shows the dynamic model of linear revolute joint used in this pantograph mechanism, according to which the following mathematical equation has been derived:

$$m\ddot{X} + K_2X - K_2Y + \mu N = 0 \tag{5}$$

$$M\ddot{Y} + (K_1 + K_2)Y - K_2X = F \tag{6}$$

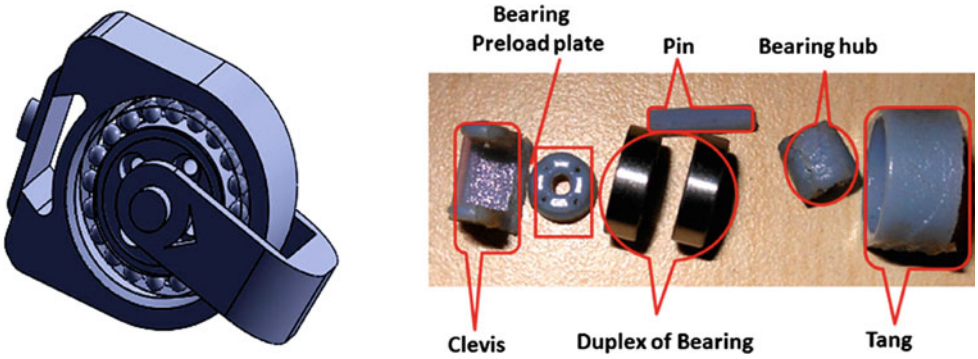

(a) *CAD model of Linear revolute joint assembly*

(b) *Revolute joints componets*

Fig. 6 Miniaturized linear revolute joint design and componets (a) CAD model of Linear revolute joint assembly (b) Revolute joints componets

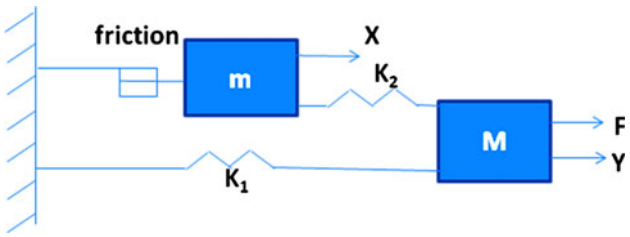

Fig. 7 Dynamic model of linear revolute joint design

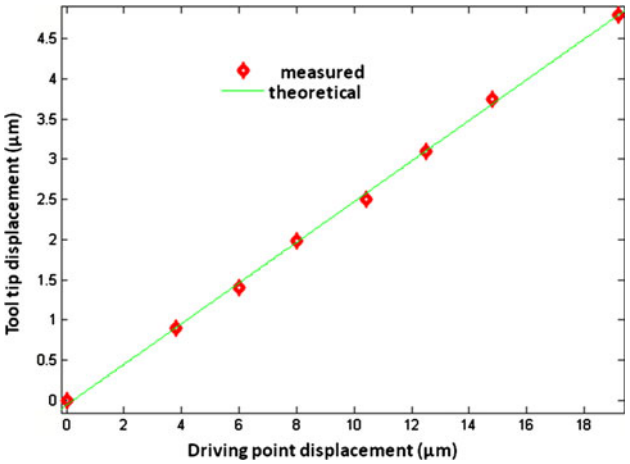

Fig. 8 Linear motion displacement comparison

where F = actuated load parameter m, M = mass parameters X, Y = displacement parameter K_1, K_2 = stiffness parameter, μ_N = friction parameter generated due to stick phenomena

3 Motion analysis

The mechanism is integrated with the symmetrically designed structural configuration. The constraints to impart desired geometric displacement have been solved through design modifications. Figure 8 compares the geometric displacements. In Fig. 8 the theoretical plot shows the simulated motion analysis performed in Solidworks. The tool tip position was measured using capacitive position sensor for every 2 µm linear motion of driving point (point of application of load by the actuator). For example, from this plot one can confirm that 16.8 µm linear motion at driving point (piezo actuator) results into 4.2 µm displacement of the tool tip along the same axis. Similarly, 3.2 µm movement of peizo actuator results in a displacement of 0.82 µm. The tool tip positional errors along Z-axis have been computed from measured data over a travel range up to 20 µm and were found to be less than 10 %, confirming the precision positioning of the tool tip with this mechanism.

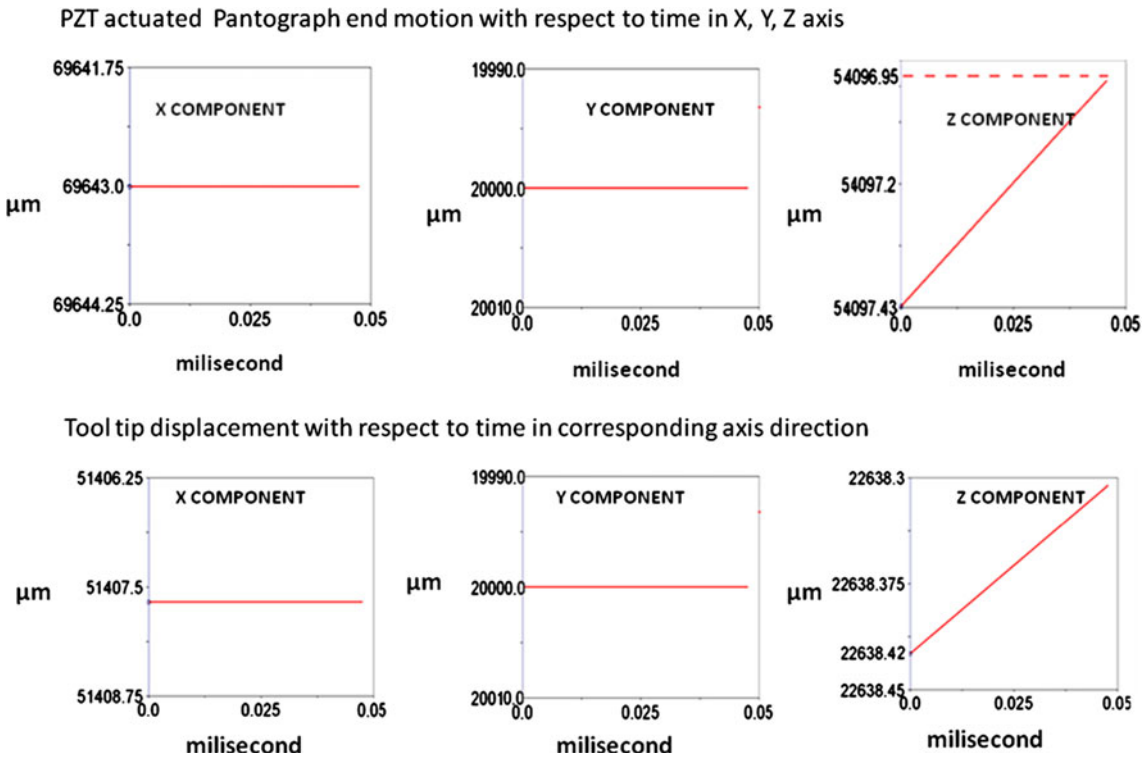

Fig. 9 ADAMS kinematic analysis results for PZT actuators movement and corresponding tool tip movement

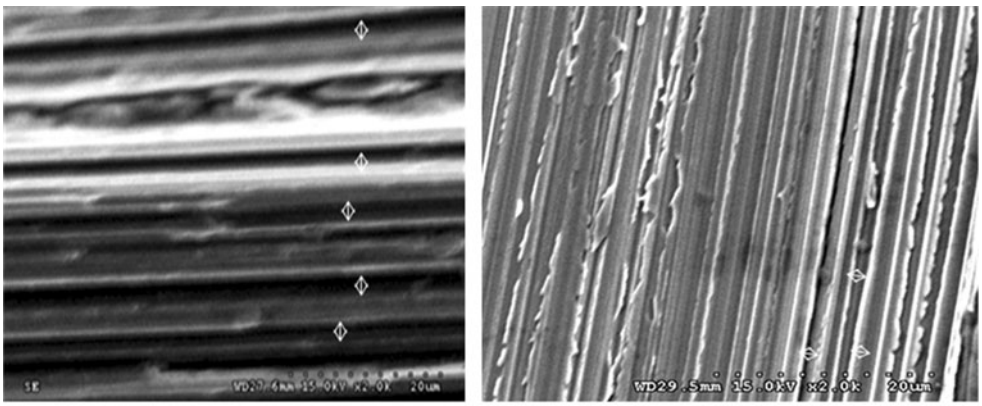

Fig. 10 Comparative study of grooves formation on Al and Cu material at scratching speed of 180 mm/min

Further, the CAD model of the Pantograph mechanism had been imported to ADAMS software and kinematic motion analysis is performed for a minimum rise time of 47 μs. Rise time is the minimum time required for the expansion of actuator. The simulation results show that for the actuated displacement of 0.48 μm through piezo-actuator, the corresponding output displacement of tool movement is 0.12 μm.

Further it is observed from the simulated plots that the mechanism could precisely move the tool in Z direction without inducing any motion in X and Y direction thus rendering the positioning to be precise as per requirements as shown in Fig. 9. It has also been observed that the resolution of the targeted motion is consistent over the entire travel.

4 Experimental demonstration

The prototype shown in Fig. 3 has been used to produce scratches over a length of 25 mm over copper and aluminium substrates. Figure 10, shows the scratches generated over Al and Cu substrates. Geometry of the scratch surface is completely dependent upon the shape of the tool i.e. trapezoidal, rectangular, and square, etc. Geometry of the surface has been observed to become slightly distorted at high speeds of the XY micro-positioning linear stage.

A comparative study of scratch on two different metals Cu and Al had been done at different operating speeds of the linearly actuated XY stages. The machine is found to operate optimally for nano scratching at low feed and high speed. Thus it may safely be summarized that the current design has the potential to be used for materials with low ductility to generate nano-scale patterns. However, repeatability and minimum resolutions that can be achieved using this mechanism are yet to be confirmed through experimental investigations, which are underway.

5 Conclusions

In this paper, a pantograph based nano-scratching machine has been designed to meet two basic functional requirements for nano-scratching of patterns over solid surfaces. The first is to impart nano-scale linear motion to the tool tip in a single axis to have better control over the depth of cut. The second target is to keep the orientation of tool tip unaltered unlike in AFM based scratching. The design analysis shows a potential reduction of linear motion by 1/4th of the driving point displacement and also ensures consistent resolution over a range of travel. Kinematic tests were conducted in MSC Adams software to analyze the feasibility of the design. Transferring high blocking forces generated by the piezoelectric actuator to tool tips enables scratching of harder surfaces. The design simulation and experimental studies have shown precision positioning of tool tip using the pantograph based mechanism. Further analysis on stiffness of the mechanism and process repeatability is being investigated.

References

1. Darzins A, Pienkos P, Edye L (2010) Current status and potential for algal biofuels production. A Report to IEA Bioenergy Task 39-T2
2. Chebolu A and Nagahanumaiah (2013) Micro-nano patterning of solid surfaces for enhanced antibacterial properties—challenges and opportunities. 1st National conference on micro and nano fabrication, CMTI Bangalore
3. Bourne K, Kapoor SG, Devor RE (2010) Study of a high performance AFM Pobe-based microscribing process, journal of manufacturing science and engineering Vol. 132/030906-1-10
4. Yoshioka H, Shinno H (2011) Design concept and structural configuration of advanced nano-pattern generator with large work area ANGEL. Int J of Autom Technol 5(1):38–40
5. Tian Y, Shirinzadeh B, Zhang D (2009) A flexure-based five-bar mechanism for micro/nano manipulation. J of Sens and Actuators A Phys 153(1):96–104

6. Howell LL (2013) Compliant mechanisms. Enclyclopedia of nanotechnology, Springer-Verlag, pp 189–216
7. Culpepper ML, Anderson G (2004) Design of a low-cost nano-manipulator which utilizes a monolithic, spatial compliant mechanism. J Precis Eng 28(4):469–482
8. Lake MS, Warren PA, and Peterson LD (1996) A revolute joint with linear load-displacement response for precision deployable structures. 37th AIAA/ASME/ASCE/AHS/ASC Structures, Structural dynamics and materials conference, salt Lake City, Utah